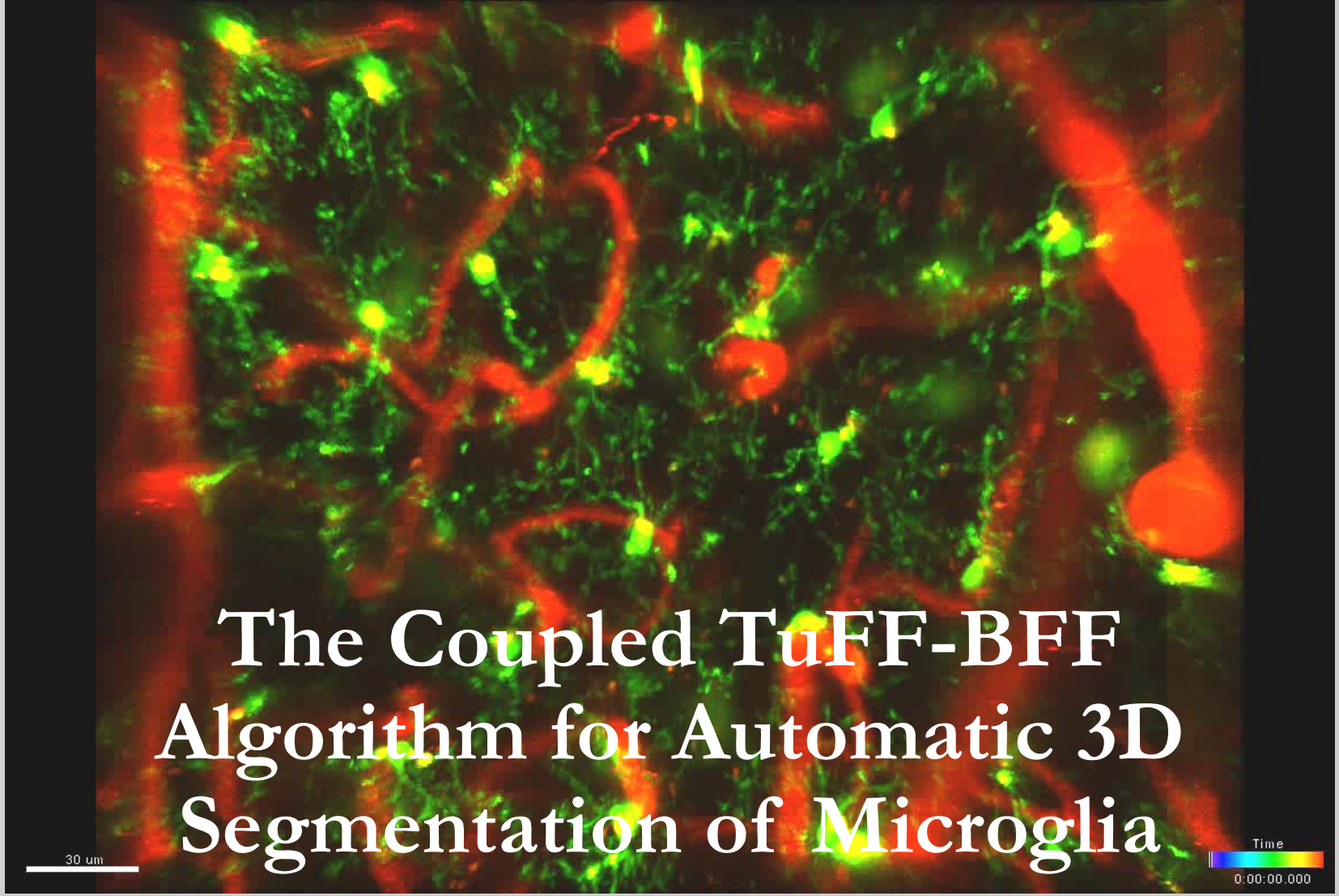

The Coupled TuFF-BFF Algorithm for Automatic 3D Segmentation of Microglia

Tiffany Ly†, Jeremy Thompson‡ , Tajie Harris‡ , and Scott T. Acton†

†Virginia Imaging and Video Analysis, C.L. Brown Electrical and Computer Engineering

‡ Center for Brain Immunology and Glia, Department of Neuroscience

Microglia

- Tissue resident macrophages, or immune cells, of the brain
- Surveillant functions: monitoring synaptic activity, sensing invading pathogens, and responding to injury

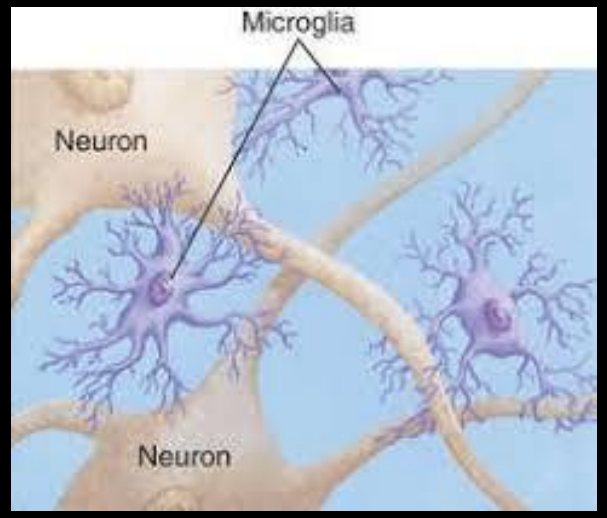

https://medical-dictionary.thefreedictionary.com/Microglial%2Bcells

Microglia

- Injuries and diseases associated with microglia:
  - Trauma
  - Stroke
  - Alzheimer's
  - Other neurodegenerative diseases

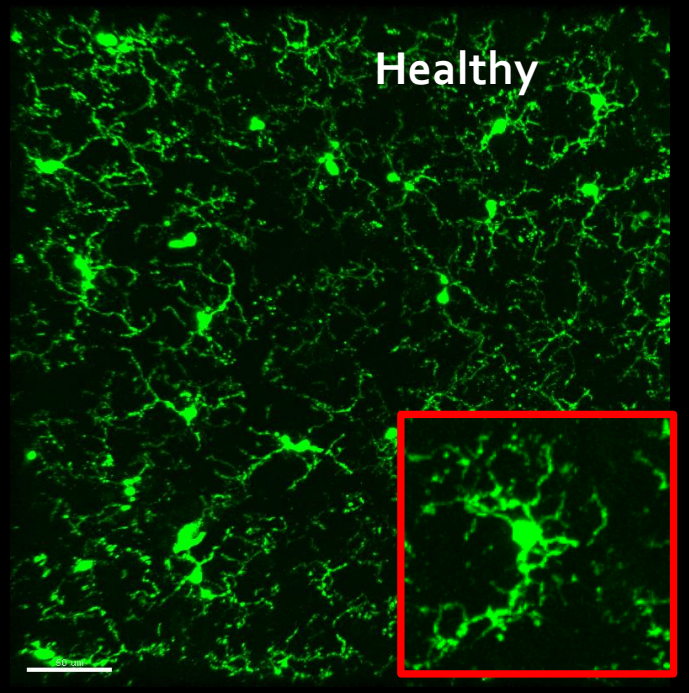

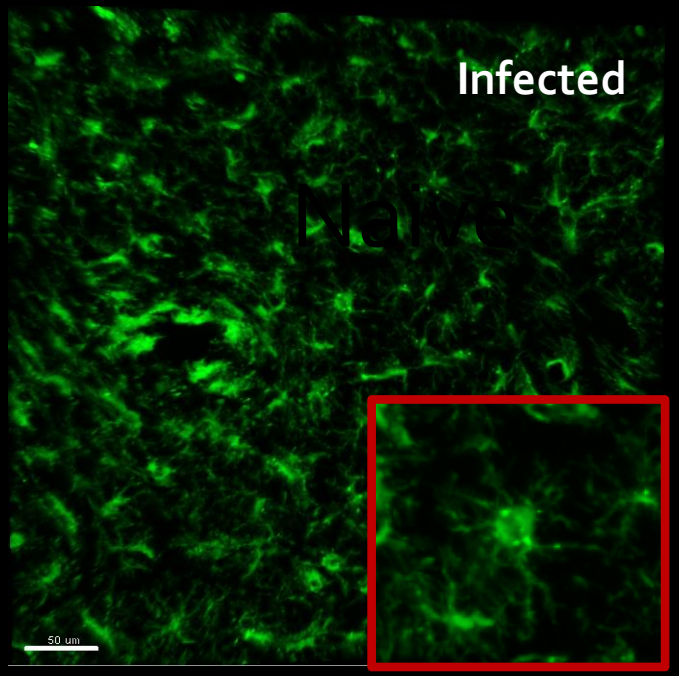

Microglia morphology and behavior are indicative of the physiological state of the brain. **Little is known about how decrease in movement affects their functionality in the brain.**

Segmentation of microglia

- Microglia have complex morphology
- Numerous 3D images → big data
- Images have intensity inhomogeneity
- Analyzing directly from grayscale is challenging

Automatic 3D segmentation technique specific to microglia!

Geometric active contour

Level Set method

$$C = \{(x)|\phi(\mathrm{x}) = 0\}$$

$$x \in \Omega, position\ in\ image\ domain$$

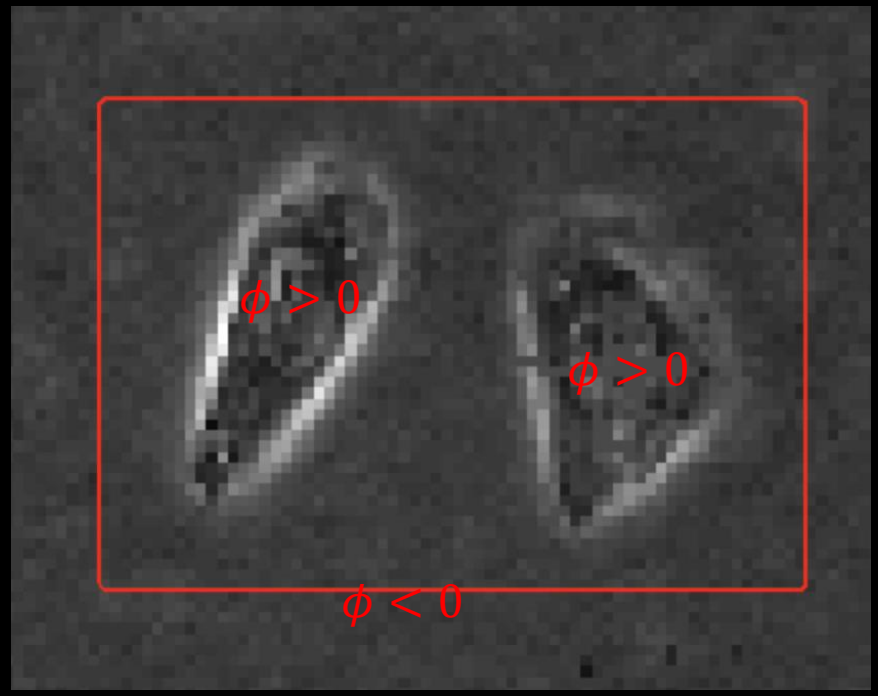

- Minimize an energy functional to evolve level set, ϕ, towards the object boundary

$$\phi = argmin\ \varepsilon\big(f(x), \phi(x)\big),$$

- Solved iteratively via gradient descent

The Coupled TuFF-BFF algorithm for 3D Segmentation of Microglia

Tubular and Blob information

- Eigenvectors of the Hessian matrix, H_ϑ, are ordered by increasing magnitude.

$$|\lambda_1| \leq |\lambda_2| \leq |\lambda_3| \gg 0$$

- Frangi's vesselness and blobness:

	λ_1	λ_2	λ_3
Vesselness	Low	High (-)	High (-)
Blobness	High (-)	High (-)	High (-)

The Coupled TuFF-BFF algorithm for 3D Segmentation of Microglia

Tubular vector flow field and Blob vector flow field

Evolve along the width and axis of contour

$$\varepsilon_{TuFF}(\phi_1) = \varepsilon_{evolve}(\phi_1) + \varepsilon_{reg}(\phi_1) + \varepsilon_{attr}(\phi_1) + \varepsilon_{repel}(\phi_1)$$

$$\varepsilon_{BFF}(\phi_2) = \varepsilon_{evolve}(\phi_2) + \varepsilon_{reg}(\phi_2) + \varepsilon_{attr}(\phi_2) + \varepsilon_{repel}(\phi_2)$$

$$\varepsilon\ \ (\phi) = -\sum_i \int_\Omega a_i(\boldsymbol{x}) \left\langle \boldsymbol{v}_i(\boldsymbol{x}), \frac{\nabla\phi(\boldsymbol{x})}{|\nabla\phi(\boldsymbol{x})|} \right\rangle^2 d\boldsymbol{x} + v_1 \int_\Omega |\nabla H(\phi)|\, dx$$

Axial vector flow field, $\boldsymbol{v_1}$

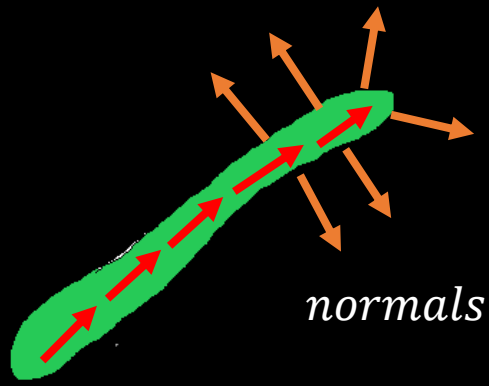

$$normals = \frac{\nabla\phi(\boldsymbol{x})}{|\nabla\phi(\boldsymbol{x})|}$$

Orthogonal vector flow fields, $\boldsymbol{v_2}$ and $\boldsymbol{v_3}$

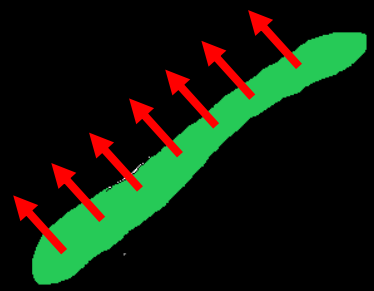

The Coupled TuFF-BFF algorithm for 3D Segmentation of Microglia

Attraction force

Connect disjoint parts

- Discontinuities caused by signal intensity loss
- Vector field from disjoint part pointed towards ROI

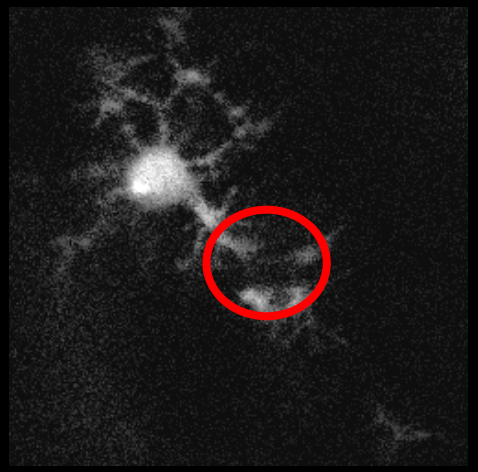

$$\varepsilon_{TuFF}(\phi_1) = \varepsilon_{reg}(\phi_1) + \varepsilon_{evolve}(\phi_1) + \varepsilon_{attr}(\phi_1) + \varepsilon_{repel}(\phi_2)$$
$$\varepsilon_{BFF}(\phi_2) = \varepsilon_{reg}(\phi_2) + \varepsilon_{evolve}(\phi_2) + \varepsilon_{attr}(\phi_2) + \varepsilon_{repel}(\phi_1)$$

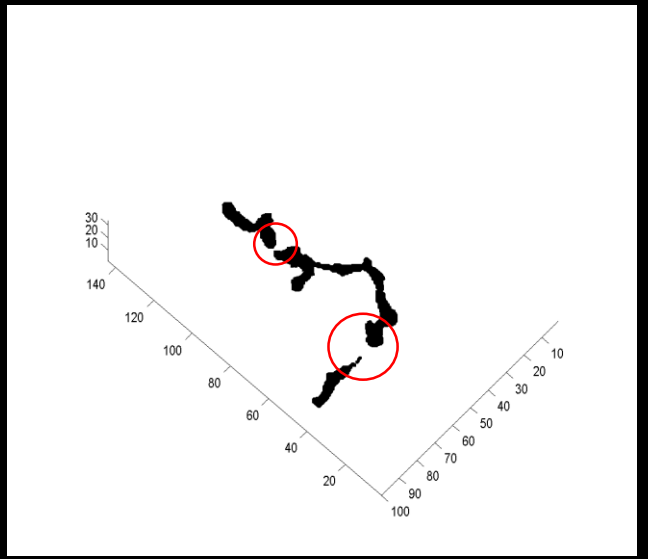

The Coupled TuFF-BFF algorithm for 3D Segmentation of Microglia

Simultaneously and separately segment tubular and blob structure to minimize overlap

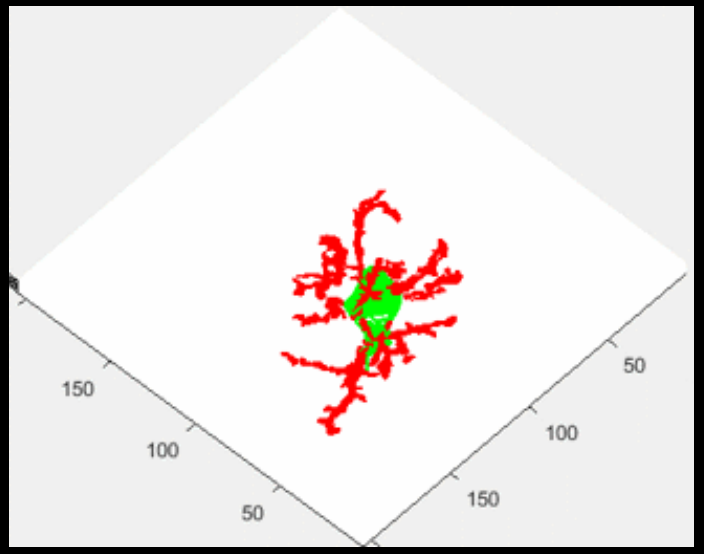

$$\varepsilon_{repel}(\phi) = \int_{\Omega} H(\phi_{TuFF}) H(\phi_{BFF}) d\boldsymbol{x}$$

$$\varepsilon_{TuFF}(\phi_1) = \varepsilon_{reg}(\phi_1) + \varepsilon_{evolve}(\phi_1) + \varepsilon_{attr}(\phi_1) + \varepsilon_{repel}(\phi_2)$$

$$\varepsilon_{BFF}(\phi_2) = \varepsilon_{reg}(\phi_2) + \varepsilon_{evolve}(\phi_2) + \varepsilon_{attr}(\phi_2) + \varepsilon_{repel}(\phi_1)$$

The Coupled TuFF-BFF algorithm for 3D Segmentation of Microglia

Minimize the energy functional by iteratively solving for ϕ with $\frac{\partial \phi}{\partial t}$, where t is time parameter. We get the velocity of the level set.

$$\frac{\partial \phi}{\partial t} = F_{reg}(\boldsymbol{x}) + F_{evolve}(\boldsymbol{x}) + F_{attr}(\boldsymbol{x}) + F_{repel}(\boldsymbol{x})$$

$$F \mathrel{+}= \frac{\partial \phi_{reg}}{\partial t} + a\frac{\partial \phi_{evolve}}{\partial t} + v_1\frac{\partial \phi_{attr}}{\partial t} + r\frac{\partial \phi_{repel}}{\partial t}$$

Segmentation results

3D images of microglia, two-photon confocal microscopy, pixel width of ~.2 μm

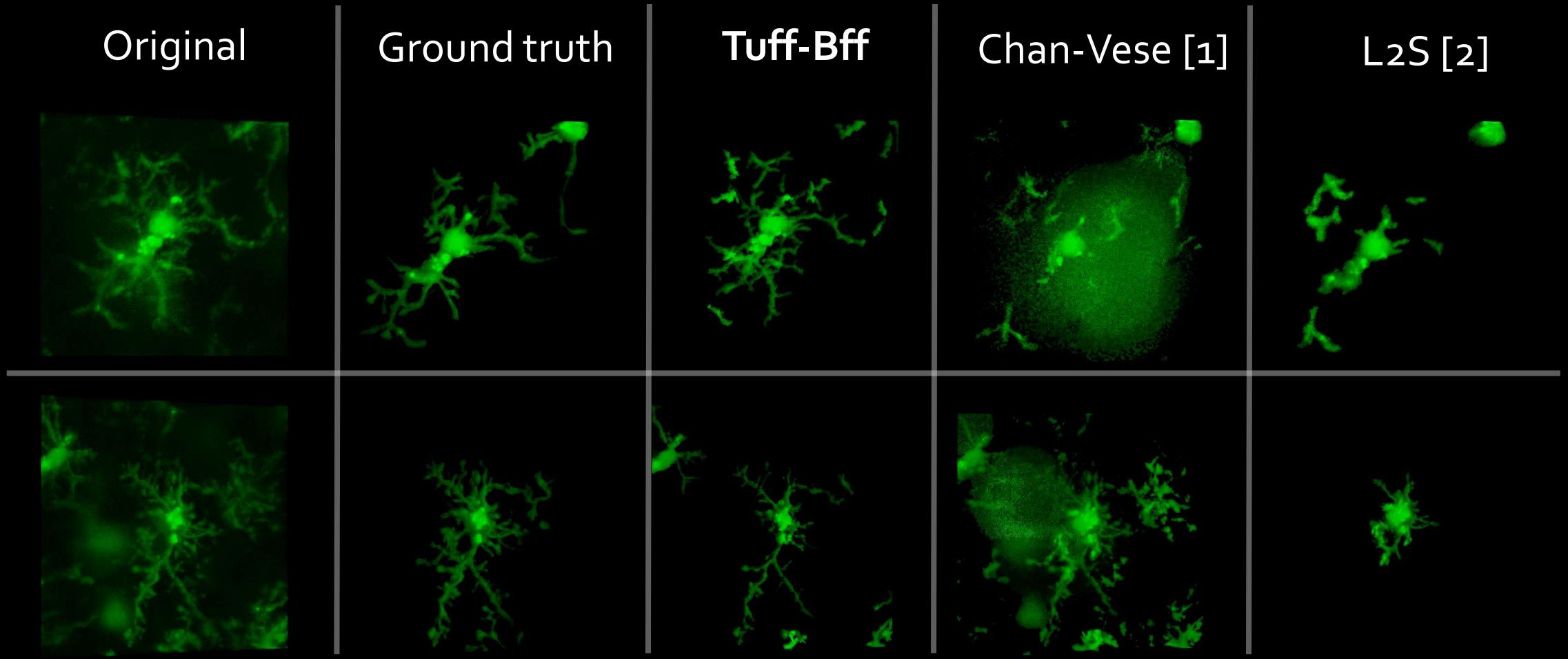

[1] T. F. Chan, *et al.*, TIP. 2001.
[2] S. Mukherjee *et al.*, SPL. 2015

More segmentation results using Tuff-Bff

Original

Segmentation

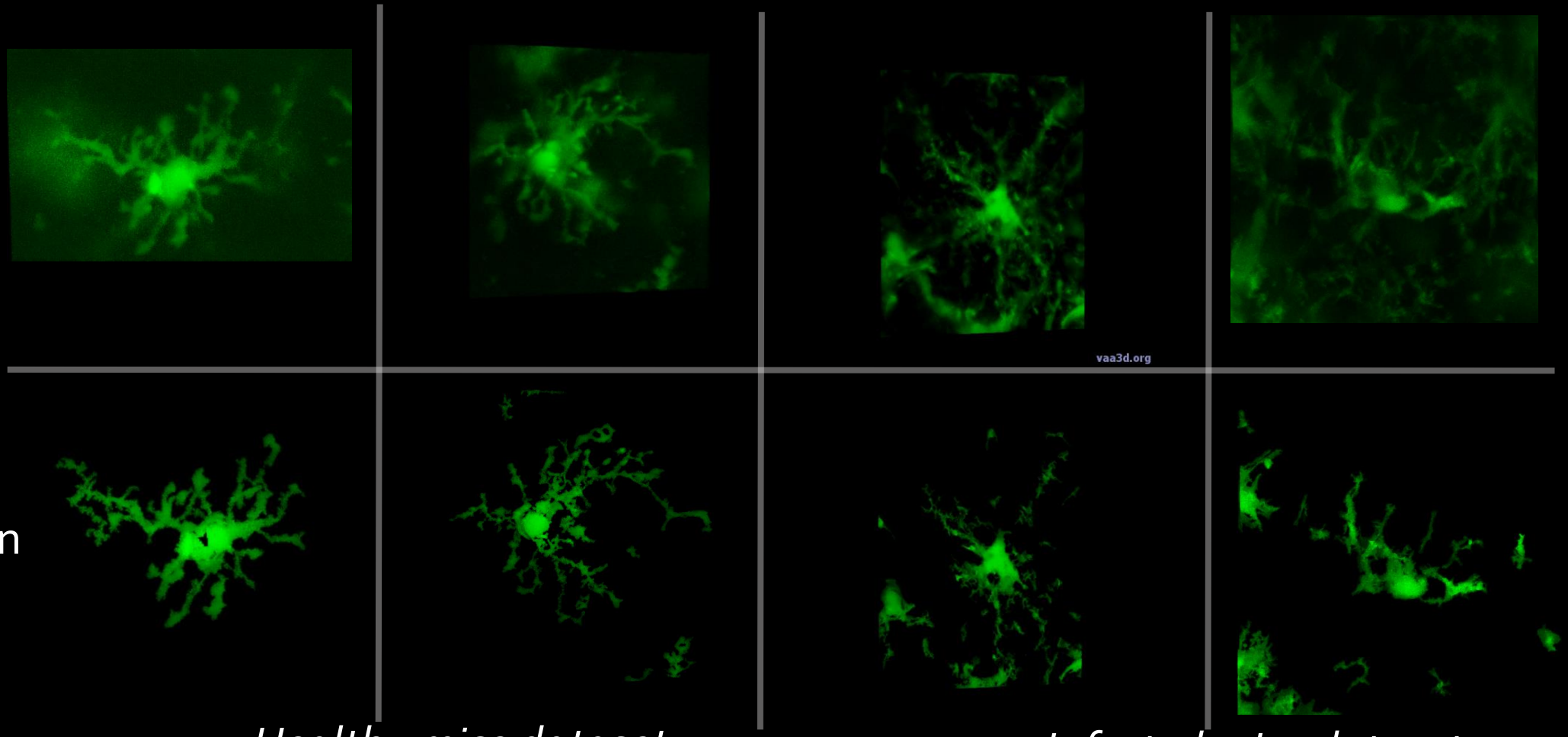

Healthy mice dataset

Infected mice dataset

Accuracy

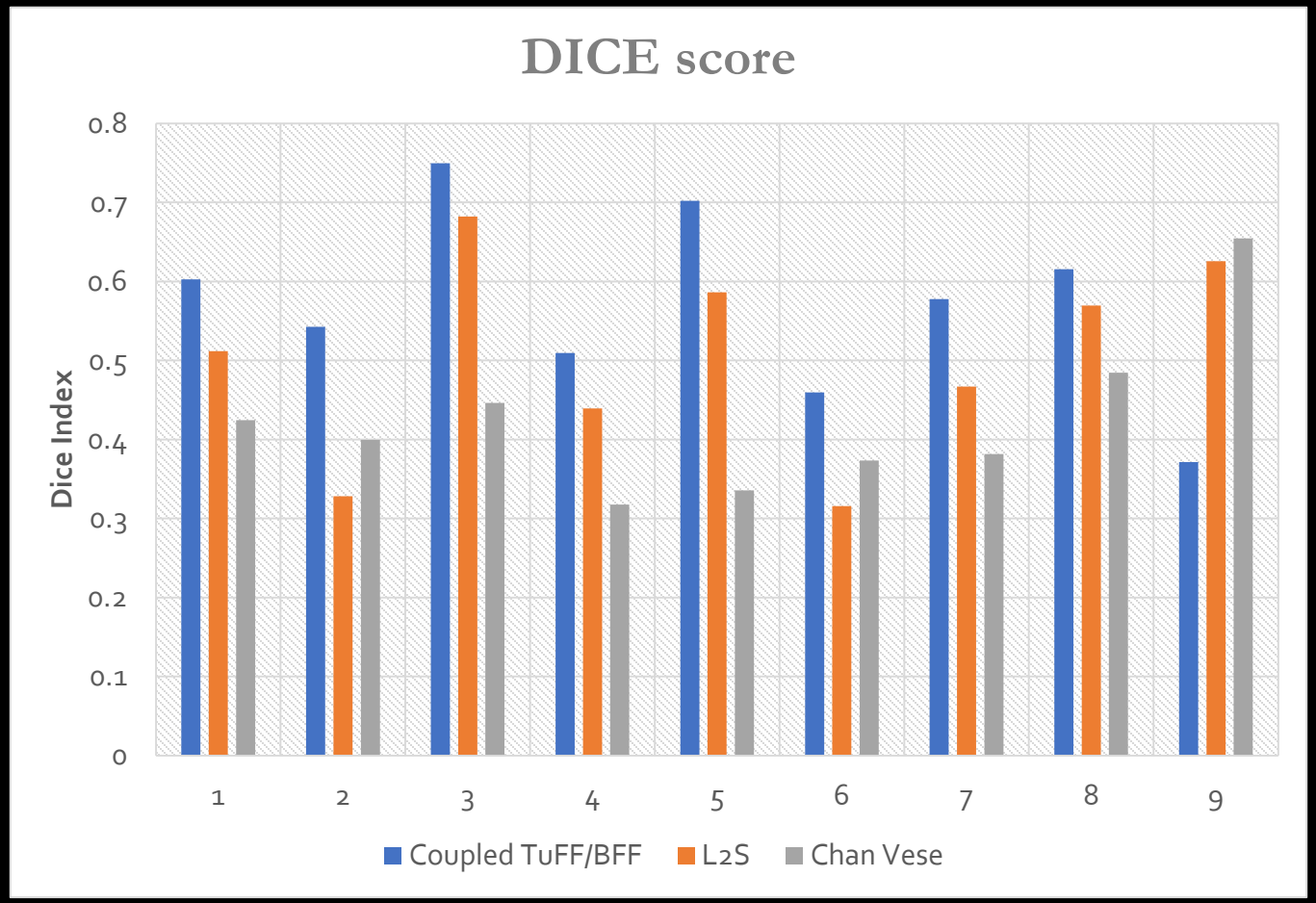

- Dice coefficient:

$$2 * \frac{|intersection(A,B)|}{|A|+|B|},$$

where A is the ground truth

- Average DICE score

Tuff-Bff: .77

Chan-Vese: .58

L2S: .53

Accuracy

Table 1 Ramification Index

No.	groundtruth	TuFF-BFF	L2S	Chan-Vese
#1	8.88	7.88	4.0	7.46
#2	7.69	10.14	2.1	9.89
#3	6.54	5.98	4.34	8.76
#4	9.02	13.6	5.48	12.4
#5	6.44	7.22	5.26	18.3
#6	8.60	8.74	3.57	11.0
#7	9.09	7.70	4.78	12.86
#8	8.88	7.88	4.0	7.46
#9	11.18	12.7	7.56	16.48
MAE:	–	1.49	3.92	3.78

- **Ramification Index** [1] : quantifies the extension of the processes from the soma

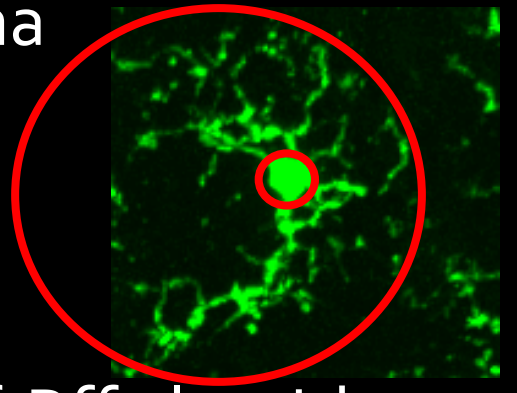

- Tuff-Bff algorithm receives the lowest mean absolute error

[1] C. Madry, *et al.*, *Neuron*, 2017

Extended Work

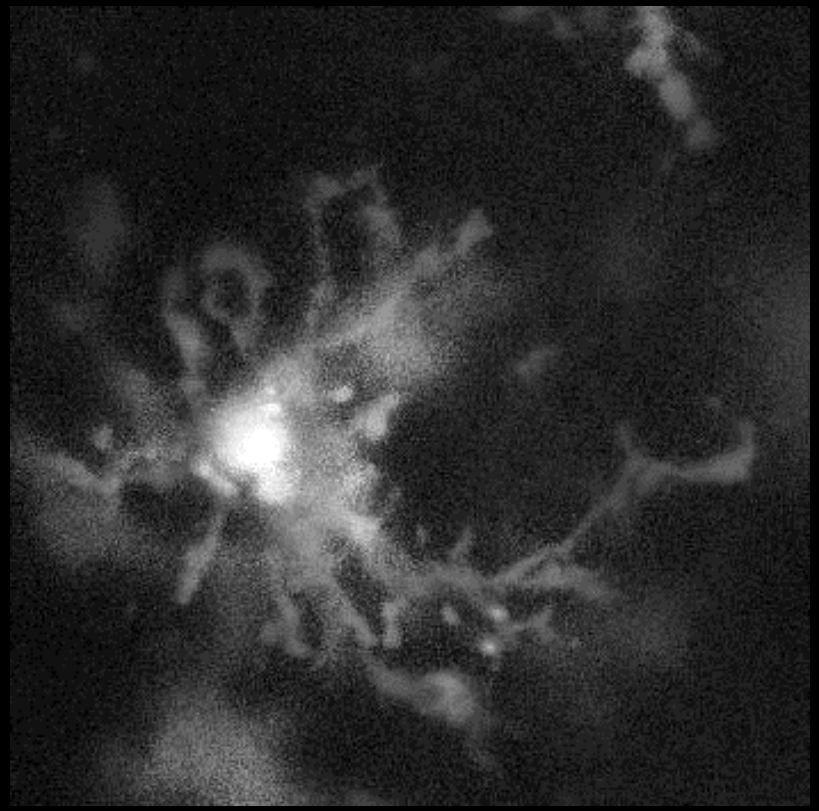

Segmentation used to create skeleton and graph

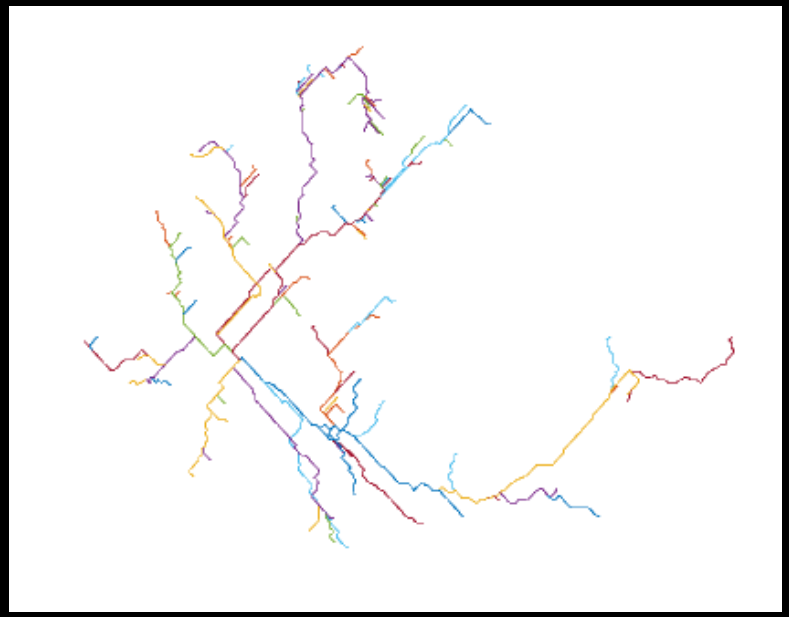

Using graph to morph glia

Via Elastic Path2Path [1]

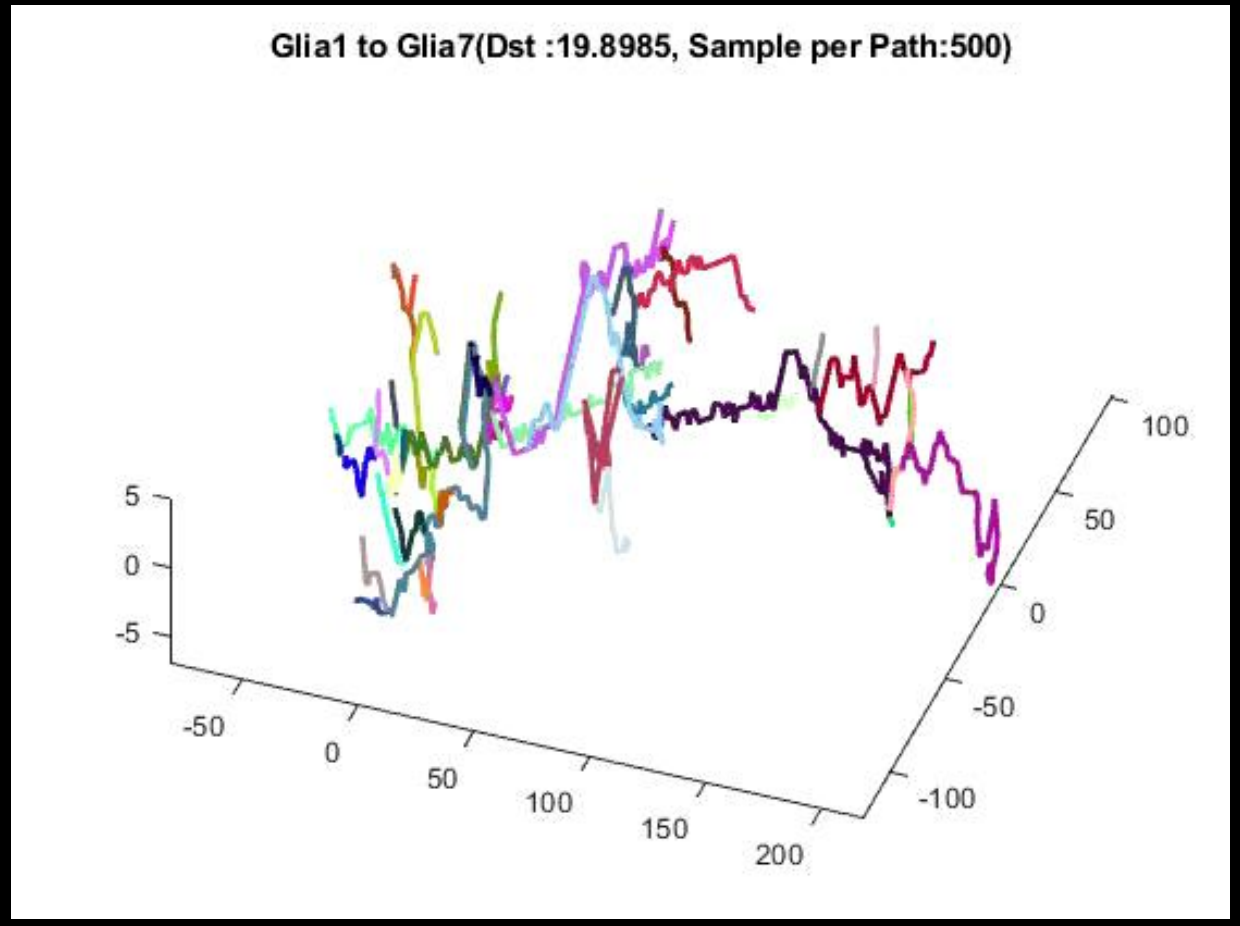

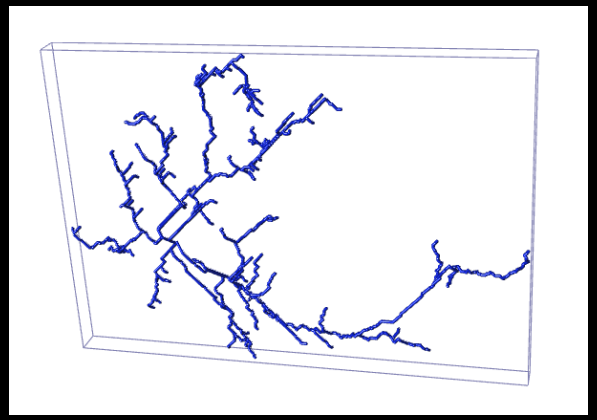

Glia 1

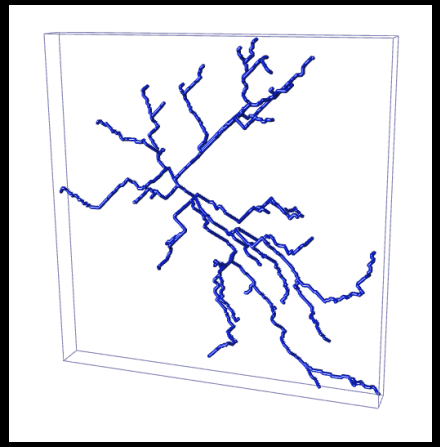

Glia 7

[1] T. Batabyal, *et al.*, ICIP. 2018

Works Cited

1. A. F. Frangi, W. J. Niessen, K. L. Vincken, and M. A. Viergever, "Multiscale vessel enhancement filtering," in International Conference on Medical Image Computing and Computer-Assisted Intervention. Springer, 1998, pp. 130–137.
2. Mukherjee, S., Condron, B., & Acton, S. T. (2015). Tubularity flow field—a technique for automatic neuron segmentation. *IEEE Transactions on Image Processing*, *24*(1), 374-389.
3. Frangi, A. F., Niessen, W. J., Vincken, K. L., & Viergever, M. A. (1998, October). Multiscale vessel enhancement filtering. In *International Conference on Medical Image Computing and Computer-Assisted Intervention* (pp. 130-137). Springer, Berlin, Heidelberg.
4. Chan, T. F., & Vese, L. A. (2001). Active contours without edges. *IEEE Transactions on image processing*, *10*(2), 266-277.
5. Mukherjee, S., & Acton, S. T. (2015). Region based segmentation in presence of intensity inhomogeneity using legendre polynomials. *IEEE Signal Processing Letters*, *22*(3), 298-302.
6. Madry, C., Kyrargyri, V., Arancibia-Cárcamo, I. L., Jolivet, R., Kohsaka, S., Bryan, R. M., & Attwell, D. (2018). Microglial ramification, surveillance, and interleukin-1β release are regulated by the two-pore domain K+ channel THIK-1. *Neuron*, *97*(2), 299-312.

Thanks